Immune checkpoint inhibitor-induced colitis is mediated by CXCR6^{+} polyfunctional lymphocytes and is dependent on the IL23/IFNγ axis

Jonathan Lo (j.lo@ic.ac.uk)
Imperial College London https://orcid.org/0000-0002-2514-9333

Domenico Cozzetto
Imperial College London

Zhigang Liu
Imperial College London https://orcid.org/0000-0002-1363-6708

Hajir Ibraheim
Imperial College London

Jillian Sieh
King's College London

Marton Olbei
Earlham Institute

James Alexander
Imperial College London

Jesus Miguens Blanco
Imperial College London

Matthew Madgwick
Earlham Institute

Hiromi Kudo
Imperial College London

Rocio Castro Seoane
Department of Immunology and Inflammation, Imperial College London

Robert Goldin
Centre for Pathology, St Mary's Hospital, Imperial College, London, UK https://orcid.org/0000-0001-5184-4519

Julian Marchesi
Imperial College London

Tamas Korcsmaros
Imperial College London

Graham Lord
University of Manchester

Nick Powell
Imperial College London

Article

Keywords:

Posted Date: January 20th, 2022

DOI: https://doi.org/10.21203/rs.3.rs-1249584/v1

Abstract

Immune checkpoint inhibitors (CPIs) have revolutionised cancer treatment, with previously untreatable disease now amenable to potential cure. Combination regimens of anti-CTLA-4 and anti-PD-1 show enhanced efficacy but are prone to off-target immune-mediated tissue injury, particularly at the barrier surfaces. CPI-induced colitis is a common and serious complication. To probe the impact of immune checkpoints on intestinal homeostasis, mice were challenged with combination anti-CTLA-4/anti-PD-1 immunotherapy and manipulation of the intestinal microbiota. Colonic immune responses were profiled using bulk and single-cell RNA-sequencing and flow cytometry. CPI-colitis was dependent on the composition of the intestinal microbiota and was characterized by remodelling of mucosal lymphocytes with induction of polyfunctional lymphocyte responses characterized by increased expression of interferon-γ (IFNγ), other pro-inflammatory cytokines/chemokines (*Il22*, *Il17a Ccl3, Ccl4* and *Ccl9*), cytotoxicity molecules (*Gzmb*, *Gzma*, *Prf1*, *Nkg7*) and the chemokine receptor *Cxcr6*. In comparison with mucosal lymphocytes in the steady state, polyfunctional lymphocytes from both $CD4^+$ and $CD8^+$ lineages upregulated costimulatory molecules and checkpoint molecules in CPI-colitis, indicating that these cells are tightly regulated. CPI-colitis was attenuated following depletion of effector lymphocytes or following blockade of the IL23/IFNγ axis. This study provides new mechanistic insights into CPI-colitis, identifying polyfunctional, cytotoxic lymphocytes as key mediators of disease. Therapeutic targeting of their effector response or regulatory networks, including the IL23/IFNγ axis likely holds the key to preventing and reversing CPI-colitis.

Introduction

Immune checkpoint inhibitors (CPIs) are highly effective immunotherapeutics that have revolutionised treatment paradigms for several cancers [1, 2, 3, 4, 5, 6]. They block inhibitory immune checkpoint molecules, such as CTLA-4 and PD-1, restoring immune activation and bolstering anti-tumour immunity. Simultaneous administration of anti-CTLA-4 and anti-PD-1 combination therapies are efficacious in advanced melanoma and renal cell carcinoma [6, 7, 8, 9]. Unfortunately, CPIs, especially in combination, also trigger off-target immune activation in non-cancer tissues causing immune-mediated organ injury, causing significant morbidity and mortality [10, 11, 12]. Diarrhoea/colitis is arguably the most important, affecting as many as 50% of CPI-treated patients and is the most common cause of serious, life-threatening complications, treatment interruption and permanent discontinuation of CPI therapy [10, 11, 12]. CPI-induced colitis is treated with high dose steroids, often for prolonged periods. Unfortunately, 40% of patients fail to respond to steroids and others develop severe complications of immunosuppression, including life-threatening infection [13, 14]. There are important concerns that immunosuppression might impede the anti-cancer responses of CPI-therapy. Two independent studies in different tumour settings, identified impaired survival in steroid exposed patients [15, 16]. Treatment outcomes with biological therapies, such as anti-TNFα drugs are also heterogeneous [17], especially if robust outcome measures are used. Not only do many patients fail to achieve steroid-free remission, but side effects also including severe infections were common [18]. Accordingly, there is a major unmet need to develop new, targeted

therapies for CPI-induced toxicity, especially as CPI therapies are increasingly deployed against additional cancer types.

Until recently, little was known about the immune characteristics of CPI-colitis. A landmark single cell sequencing experiment identified expansion of T cells in CPI colitis with activation of both $CD4^+$ and $CD8^+$ populations, including upregulation of cytolytic programmes and increased expression of interferon-γ (IFNγ) [19]. A second study focussing on $CD8^+$ cells replicated these findings and identified expansion of tissue resident populations as key cytokine producing cells [20]. There is now a pressing need for mechanistic insights to understand the critical immune drivers and regulators of CPI-colitis to inform the development of targeted therapies.

Results

The composition of the intestinal microbiota regulates susceptibility to immune checkpoint inhibitor-induced colitis

To understand how immune checkpoint perturbation impacts the colonic immune system, we administered anti-CTLA-4/anti-PD-1 combination therapy to wild type (WT) Balb/C mice. Although checkpoint inhibition alone triggered systemic immune activation with induction of splenomegaly, there was no change in colonic mass of treated with immune checkpoint inhibitors (CPIs) (Figs. 1A and B). Since intestinal microbiota influences colitis susceptibility in cancer patients treated with CPI [21, 22, 23, 24], we investigated whether altering the intestinal microbiota impacted colitis susceptibility. To test this hypothesis, we transplanted the caecal microbiota harvested from TRUC mice, that are colonized with a pro-inflammatory microbiota [25, 26] to WT mice. Although faecal microbiota transplantation (FMT) by itself did not induce colitis, subsequent challenge with combination anti-CTLA-4/anti-PD-1 therapy did (Figs. 1A and B). We observed increased colon mass and failure to gain weight gain in recipients of combination anti-CTLA-4/anti-PD-1 and FMT (Figs. 1A-C). Histological assessment of the colon demonstrated relatively mild changes in mice receiving combination CPI and FMT, including although features consistent with reports of CPI-colitis in patients, with increased lymphocytes in the colonic lamina propria, increased intraepithelial lymphocytes and increased epithelial apoptosis (Fig. 1D and Supplementary Figs. 1A and B). Colonic lymphocyte expansion was corroborated by flow cytometry with increased infiltration with both $CD4^+$ and $CD8^+$ T cells in the lamina propria of mice treated with combination anti-CTLA-4/anti-PD-1 and FMT (Figs. 1E-G).

Neutrophil accumulation in the colon is a key feature of CPI-colitis [27], therefore, we also evaluated the colonic myeloid compartment. There was also significant accumulation of $CD11b^+$ $Gr\text{-}1^{high}$ neutrophils and $Ly6C^{high}$ MHC class II^- inflammatory monocytes in the colon of mice treated with FMT and CPI

(Figs. 1H and I and Supplementary Figs. 2A-C). Disease could also be induced in C57BL/6 mice (Supplementary Fig. 2D), indicating that this phenomenon was mouse strain independent.

Changes in the intestinal microbiota induced by FMT were recorded using 16S rRNA amplicon sequencing. There was no significant change in α-diversity following FMT (Shannon index 2.19 in control vs 2.40 in FMT group P=0.24, Supplementary Fig. 3A); however, β-diversity was significantly different between control and FMT groups (P=0.038, Supplementary Fig. 3B). At phylum level, there were no differences between control mice or FMT recipients (Supplementary Fig. 3C). However, at family level, *Rikenellaceae*, *Prevotellaceae* and *Desulfovibrionaceae* were more abundant in the FMT samples compared to untreated controls, while *Tannerellaceae* and *Muribaculaceae* were significantly reduced (Supplementary Fig. 3D). At genus level, *Alistipes* and *Rikenella* RC9 gut group were significantly more abundant in FMT samples. By contrast, members of the *Parabacteroides* and *Muribaculaceae* genera were significantly more abundant in control samples (Supplementary Fig. 3E).

Transcriptomic profiling demonstrates colonic epithelial dysfunction, interferon signalling and cytotoxicity in CPI-colitis

To investigate the immunopathology of this model of CPI-induced colitis, we analysed gene expression changes in the distal colon using bulk RNA-sequencing. There were only minor transcriptional changes observed in mice treated with CPI only (Fig. 2A). However, following FMT, transcriptomic variation was also moderate, although we did observe significant induction (FDR < 0.05) of genes involved in humoral immunity, such as the activation-induced cytidine deaminase gene (*Aicda*), which plays a critical role in somatic hypermutation and class switching in B cells activated in response to microbial challenge [28], and over-expression of immunoglobulin chains, including selective variable regions (*Ighg2b, Igkv8-21, Igkv4-61*) (Supplementary Fig. 4A). Biological pathway analysis (IPA, QIAGEN) identified three causal networks associated with the gene expression changes induced by FMT that were merged into a single network, additionally identifying IFNγ and TNFα as key nodes (Supplementary Fig. 4B).

Transcriptomic changes were more pronounced in FMT and combination CPI treated mice, with a greater number of differentially expressed genes (DEGs) and a greater magnitude of the differences, including 385 transcripts significantly affected (FDR<0.05), of which 258 showed at least doubled expression levels and 22 at least halved (Fig. 2A and B). The most significantly upregulated transcripts encoded proteins involved in epithelial barrier function, extracellular matrix regulation and anti-microbial responses. The most prominent upregulated transcripts included multiple members of the late cornified envelope (LCE) gene cluster and keratin family genes (Fig. 2C). Their expression is dysregulated in barrier surface diseases in response to tissue injury and infection [29, 30, 31]. Expression of other genes involved in epithelial function, including defensins, aquaporins and were also dysregulated, as is observed in conventional IBD [32]. Other upregulated genes included interferon stimulated genes (e.g. *Nos2*, *Isg15*, *Ifit2*, *Gbp3* and *Gbp7)*, molecules involved in cell-mediated cytotoxicity (*Gzma, Gzmb, Tnf*), proteases and their inhibitors (*Ctsc, Srgn, Serpina12, Serpina3c*) and molecules involved in antigen processing/presentation (*Cd74* and multiple MHC molecules) (Figs. 2B and C).

Biological pathway analysis identified significant enrichment of biological processes, such as interferon signalling, T cell exhaustion, dendritic cell maturation, death receptor signalling and activation of phospholipase C and p38 MAP kinase in CPI-colitis (Fig. 2D). Causally affected processes (Downstream Effects Analysis, IPA, QIAGEN) predicted to be significantly activated (z-score>2, FDR<0.05) in CPI-colitis included systemic autoimmune syndrome, anti-microbial response, activation of leukocytes, cytolysis, and activation of cytotoxic T cells (Fig. 2E). Causal network analysis of the most enriched pathway (systemic autoimmune syndrome) identified a complex interplay of cytokines, chemokines, antigen processing/presenting molecules, cytotoxicity molecules, myeloid molecules, and transcription factors (Supplementary Fig. 5A).

We found multiple predicted upstream regulators of the molecular changes observed in the colon in CPI-colitis, including cytokines (IFNγ, IL1β, IL6, IL21, IL27 and TNFα), microbial products/TLR agonists (LPS, TLR3, TLR4, CpG, MyD88) and transcription factors (NFκB, CEBPB, NFATC2) (Fig. 2F). Immunosuppressive drugs, including etanercept (an anti-TNFα agent), sirolimus, and the immunosuppressive cytokines IL10 and SOCS1 were predicted inhibitors of the gene expression changes observed in CPI-colitis. The cytokine predicted to be most highly activated in CPI-colitis was IFNγ (z-score= 6.6, FDR=$2.06x10^{-23}$) (Fig. 2F). Network analysis of its interactions with the DEGs identified a range of biological processes regulated, including antigen presentation, oxidative stress, chemokine induction, JAK/STAT signalling, and proteasome activation (Supplementary Fig. 6A).

To determine whether this model of CPI-colitis mirrored aspects of human disease, we evaluated the similarity between the transcriptional differences observed in our model and those reported in cancer patients developing combination CPI-colitis [33]. Consistent with our model recapitulating gene expression changes in human CPI-induced colitis, gene set enrichment analysis (GSEA) demonstrated that the mouse homologs of the most significantly up-regulated genes probed in patients were among the most over-expressed ones in our model (Supplementary Fig. 7A).

High resolution single cell transcriptomics reveals colonic lymphocyte remodelling and emergence of polyfunctional, cytolytic lymphocyte responses in CPI-induced colitis

To further probe immune mechanisms of CPI-induced colitis, we performed single cell RNA-sequencing (scRNA-seq) from FACS purified live $CD45^+$ lymphocytes from the colons of mice with CPI-colitis and control mice. Cluster analysis demonstrated shifts in the proportional abundance of colonic lymphocyte populations, including expansion of T cell clusters 1, 4, 6, 24, B cell clusters 3 and 8, and ILC cluster 22 (Figs. 3A-D, Supplementary Fig. 8A).

Analysis of the main lymphocyte lineages identified remodelling of the transcriptome in T cells, B cells and ILCs (Figs. 3B-D). There was significant upregulation (Bonferroni corrected P-value <0.001) of *Ifng*, *Gzmb*, *Gzma, Nkg7*, and the chemokines *Ccl3*, *Ccl4* and *Ccl5* in T cell compartment in CPI-induced colitis (Fig. 3B). In T cells, Canonical Pathway Analysis (IPA, QIAGEN) identified significant enrichment of biological processes including T_H1 and T_H2 activation, cytotoxicity, and T cell exhaustion in CPI-colitis

(Fig. 3B). In B cells, there was upregulation of transcripts involved in protein synthesis and endoplasmic reticulum stress, such as *Calr*, *Hspd1*, *Hspa5*, in keeping with B cells adopting a secretory state in CPI-induced colitis (Fig. 3C). In B cell clusters the most upregulated biological pathways were antigen presentation pathways, and pathways linked to immune-mediated inflammatory diseases, including SLE and GvHD (Fig. 3C). In ILCs there was also upregulation of cytotoxicity molecules, such as *Gzma*, *Gzmb*, *Gzmc* and *Prf1*, and the cytokines/chemokines *Il22* and *Ccl3* (Fig. 3D). In ILCs, crosstalk between NK cells and DCs, and cytotoxicity signalling pathways were enriched (Fig. 3D).

Cluster-specific analysis of lymphocytes in CPI-colitis demonstrated expression of *Ifng* across multiple T cell clusters, including *Cd4*$^+$ clusters 4, 6 and 9, *Cd8*$^+$ clusters 24 and 25, and ILC clusters 16 and 22 (Fig. 3E). These clusters also expressed high levels of cytotoxicity molecules (*Gzma*, *Gzmb*, *Prf1* and *Nkg7*), chemokines (*Ccl3*, *Ccl4* and *Ccl5*), both subunits of the IL12 receptor heterodimer (*Il12rb1* and *Il12rb2*), and *Cxcr6*, *Tnfrsf9* and *Stat1* (Fig. 3E and Supplementary Fig. 8B).

IFNγ producing CD4$^+$ and CD8$^+$ T cell populations co-express multiple pro-inflammatory cytokines and cytotoxicity molecules in CPI-colitis

Given the prominent IFNγ footprint observed in CPI-colitis, we further probed the transcriptome of *Ifng*-expressing lymphocytes in CPI-colitis in comparison with their *Ifng*-expressing counterparts in control mice. As well as being expanded in CPI-colitis, *Ifng*-expressing lymphocytes co-expressed Gzmb (Fig. 4A and B). In comparison with *Ifng*-expressing CD4$^+$ T cells in control mice, the top 20 most highly upregulated transcripts in *Ifng*-expressing CD4$^+$ T cells in CPI colitis, included chemokines (*Ccl3, Ccl4, Ccl5, Ccl9*), other cytokines (*Il22, Il13, Il17f, Il10, Spp1*), and cytotoxicity molecules (*Gzma, Gzmb, Prf1, Nkg7*) (Fig. 4C). In CPI colitis, *Ifng*-expressing CD8$^+$ T cells upregulated a similar pattern of transcripts, with increased expression of other cytotoxicity molecules, chemokines, and cytokines among the most highly upregulated 20 transcripts (albeit with a more limited repertoire of cytokines than CD4$^+$ T cells, Fig. 4C). The most highly upregulated transcript in *Ifng*-expressing ILCs in CPI-colitis was *Il22*, and cytotoxicity molecules were again among the most highly expressed transcripts in these cells (Supplementary Fig. 9A).

To determine whether these changes were observed at protein level, we performed flow cytometry. An increased proportion of colonic T cells co-expressing IFNγ and cytotoxicity molecules, such as granzyme B and perforin was observed in CPI-colitis, especially in CD4$^+$ and CD8$^+$ T cells (Figs. 4D and E, Supplementary Fig. 9B and C), and to a lesser extent CD3$^-$ IL-7R$^+$ cells (Supplementary Fig. 9D).

We investigated which biological pathways were enriched in *Ifng*-expressing lymphocytes using the Canonical pathways tool (Ingenuity). The top 20 most enriched, overlapping canonical pathways in *Ifng*-expressing CD4$^+$ T cells in CPI colitis in comparison with *Ifng*-expressing lymphocytes in control mice included TCR and co-stimulatory molecule activation, effector lineage activation (Th1, Th2 and Th17 pathways), coronavirus signalling pathways and metabolic reprogramming, including oxidative phosphorylation (Fig. 4F and Supplementary Fig. 10A). Other important pathways that were significantly

activated in these cells included ICOS-ICOSL signalling in Helper T cells (z-score =2.53, P<3.3 x10^{-5}), OX40 signalling pathway (z-score =1.89, P<3.3 x10^{-5}) cross talk between DCs and NK cells (Z-score 2.53, P<0.0013) and the IL23 signalling pathway (z-score=2.45, P<0.032). There was a very similar pattern of Canonical Pathways activated in *Ifng*-expressing $CD8^+$ T cells in CPI colitis in comparison with *Ifng*-expressing lymphocytes in control mice (Supplementary Fig. 10B).

To determine whether IFNγ was functionally important in CPI colitis we administered neutralizing anti-IFNγ monoclonal antibodies, or isotype matched control antibodies, to mice during induction of CPI-colitis. Antibodies were administered simultaneously at the same time as combination CPI at weeks 0, 1 and 2. In keeping with IFNγ playing an important role in CPI colitis, neutralization of this cytokine significantly reduced colon mass in anti-IFNγ treated animals (Fig. 4G).

IFNγ producing lymphocytes have increased expression of co-stimulatory and immune checkpoint molecules

To further analyse the phenotype of IFNγ producing lymphocytes in CPI-colitis, we examined their expression of co-stimulatory molecules, co-inhibitory molecules, chemokine receptors and gut homing integrins. In both $CD4^+$ and $CD8^+$ T cells, there was an increase expression of co-stimulatory molecules in IFNγ producing lymphocytes in CPI-colitis. In $CD4^+$ T cells this included classical co-stimulatory molecules, such as *Cd28* and *Cd2*, and numerous members of the TNF receptor superfamily, including *Tnfrsf4*, *Tnfrsf18* and *Tnfrsf9* (Fig. 5A) There was a similar pattern of co-stimulatory molecule upregulation in $CD8^+$ T cells, although CD27 was the most upregulated receptor in these cells (Fig. 5A). In CPI-colitis, IFNγ producing lymphocytes also upregulated co-inhibitory receptors. In $CD4^+$ T cells, the most upregulated checkpoints molecules, included *Ctla4* (fold change = 2.2, FDR=7.0x10^{-46}), *Hacvr2* (Tim-3, fold change 1.8, FDR=3.7 x10^{-58}) and Lag3 (fold change = 1.7, FDR=1.2 x10^{-38}). A broadly similar pattern was observed in $CD8^+$ T cells with *Hacvr2* (fold change 2.6, FDR=1.8 x10^{-61}) and *Lag3* (fold change = 2.5, FDR=6.7 x10^{-27}) being the most upregulate checkpoint molecules (Fig. 5A and Supplementary Fig. 11A). These data imply that both $CD4^+$ and $CD8^+$ IFNγ producing lymphocytes are very tightly regulated in CPI-colitis.

To evaluate the functional role of these activated lymphocytes in CPI-colitis we took advantage of antibodies that deplete CD90 expressing cells. Although CD90 is often regarded as a pan-T cell marker, it is also a potent co-stimulatory molecule, and its ligation imparts a potent activation signal to T cells [34]. Like other activation markers, the expression of CD90 increased in *Ifng* expressing $CD4^+$ and $CD8^+$ T cells (Fig. 5A). Similar findings were observed at protein level, with upregulation of CD90 in both $CD4^+$ and $CD8^+$ T cells after induction of CPI-colitis (Fig. 5B and C). Consistent with a more activated phenotype, cells with the highest expression of CD90 produced more cytokine, including a population of dual IFNγ and TNFα producing cells, in both $CD4^+$ and $CD8^+$ T cells (Fig. 5D and Supplementary Fig. 12A). Administration of depleting anti-CD90 antibodies significantly reduced the number of $CD3^+$ $CD90^+$ T cells

in the colon following induction of CPI colitis and significantly attenuated disease, with reduced colon mass and abrogation of excessive neutrophil recruitment (Figs. 5E-H).

To further evaluate the phenotype of *Ifng*-expressing lymphocytes in CPI colitis, we compared chemokine and gut homing receptors in cells in comparison with lymphocytes that do not express *Ifng.* In both $CD4^+$ cells and $CD8^+$ T cells, the most upregulated chemokine receptor was *Cxcr6 (*6.3-fold, FDR=$2.1x10^{-105}$ in $CD4^+$ T cells and 2.2-fold, FDR, and 3.6-fold, $1.1x10^{-19}$ in $CD8^+$ T cells), and in the case of $CD8^+$ T cells, *Cxcr6* was the only upregulated chemokine receptor (Fig. 5I and Supplementary Figs. 13A and B). Gut homing receptors, including *Itga4* and *Itgb7* that encode the classical gut homing integrin heterodimer α4β7 was downregulated in both *Ifng*-expressing $CD4^+$ and $CD8^+$ lymphocytes. These data maybe consistent with the hypothesis that tissue resident cells, or cell arising from tissue resident cells, are key drivers of CPI colitis rather than newly recruited T cells, especially since CXCR6 was the most highly upregulated chemokine receptor in both $CD4^+$ and $CD8^+$ lymphocytes. Notably, markers of tissue resident memory lymphocytes, including CD103 and CD69 were not upregulated in *Ifng*-expressing lymphocytes. To determine whether *de novo* recruitment of lymphocytes is required to initiate colitis, we administered anti-integrin α4β7 mAbs to mice prior to, and during, induction of CPI-colitis. Although anti-integrin α4β7 mAbs substantially reduced the number of integrin α4β7 expressing T cells in the colon and mesenteric lymph nodes (Fig. 5J), it failed to prevent or even reduce the severity of CPI-colitis (Figs. 5K and L). These data are consistent with an important pathogenic role of $CXCR6^+$ lymphocytes likely arising from tissue resident memory cells, rather than lymphocyte populations that have been newly recruited to the gut.

IL23 blockade suppresses IFNγ-producing CD4+ colonic T cells and attenuates the development of CPI-colitis.

There is a major unmet need to identify therapeutically tractable mediators in CPI colitis, therefore, we conducted an Enhanced Causal Network Analysis (IPA) to identify upstream mediators responsible for activating the pattern of gene expression that we observed in *Ifng* expressing lymphocytes in CPI colitis. Analysis of cytokines predicted to activate *Ifng* expressing $CD4^+$ T cells in CPI colitis included IL2 (z-score 4.7, P<$1.0x10^{-27}$), IL7 (z-score 3.8, P<$9.8x10^{-19}$), IL15 (z-score 3.4, P<$5.2x10^{-34}$), IL18 (z-score 2.0, P<$4.0x10^{-25}$) and IL23A (z-score 2.6, P<$2.1x10^{-31}$) (Fig. 6A, Supplementary Table 1). Other predicted regulators included transcriptional regulators (TBX21, NFATC2, STAT3, IRF6 and IRF9) and transmembrane receptors, including co-stimulatory molecules (CD244), cytotoxicity receptors (NKG2D), CD69 and the complement receptor CD46 (Fig. 6A, Supplementary Table 1).

From a therapeutic perspective targeting cytokines predicted to activate these pathogenic cells is an attractive strategy, as many neutralizing monoclonal antibodies have been, or are currently, in clinical development for other immune-mediated inflammatory diseases. IL23 is an especially attractive target in CPI-colitis with multiple reagents is advanced development to treat conventional inflammatory bowel diseases. To determine whether IL23 is functionally important in CPI-colitis, we administered mAbs that neutralize p19 subunit of the IL23 heterodimer, or isotype matched control antibody at the same time as

combination immunotherapy. IL23 blockade reduced the number of IFNγ producing $CD4^+$ T cells in the colon in CPI-colitis and especially IFNγ/TNFα co-producing cells (Figs. 6B and C). The proportion of cytokine producing $CD8^+$ T cells were unaffected by the blockade of IL23 (Supplementary Figs. 14A and B). IL23 blockade attenuated key disease features, including significantly reduced colon mass and reduced recruitment of colonic neutrophils (Figs. 6D and E). These data were corroborated by inducing CPI-colitis in *Il23*$^{-/-}$ mice, with reduced colon mass and reduced numbers of infiltrating neutrophils in comparison with WT littermate control mice (Figs. 6F and G). Furthermore, $CD4^+$ T cells also had reduced number of IFNγ/TNFα co-producing cells (Fig. 6H and I). Proportions of $CD8^+$ T cells were again unaffected by the genetic ablation of *Il23* (Supplementary Figs. 14C and D). Together these data are consistent with IL23 playing an important role regulating the evolution of pathogenic effector $CD4^+$ T cells in CPI-colitis and identify IL23 as a potentially important therapeutic target in CPI-colitis.

To investigate whether IL23 could be a viable target in human CPI-induced colitis we interrogated a gene expression in the colon from a recently published dataset of patients developing CPI-colitis following treatment with combination immunotherapy. Consistent with our analyses there was significant upregulation of cytotoxicity molecules (*PRF1, GZMB*, *GZMA*) and interferon-responsive genes (*CXCL10*) (Fig. 6J). There was also significant upregulation of *IL23* and its key signalling molecule *STAT3*, indicating that IL23 is likely to be a viable therapeutic target in CPI-colitis.

We constructed a regulatory network predicted to be activated by IL23 based on downstream gene expression changes in *Ifng* expressing $CD4^+$ T cells, which identified activation of transcription factors (STAT3, NFATC1), MAP kinase pathways (ERK1/2, p38 MAPK), signalling molecules (Phospholipase C gamma 2) and other kinases (PRKCD, Syk) implicated in inflammatory diseases (Fig. 6K). Together our data support the rationale for therapeutic targeting of IFNγ producing, polyfunctional T cells in CPI colitis, including neutralization of their upstream regulators, such as IL23.

Discussion

This study provides mechanistic insights into the immunopathogenesis of CPI-induced colitis and identifies polyfunctional mucosal $CD4^+$ and $CD8^+$ T cells that co-produce IFNγ, other pro-inflammatory cytokines (e.g. IL22, IL17A) and cytolytic molecules, including granzyme B, as key effector cells in CPI colitis. These cells are activated and expanded in the colon in CPI-colitis. These pathogenic, polyfunctional T cells resemble T cell populations implicated in anti-viral responses and anti-tumour immunity, and importantly also recapitulate studies describing the phenotype of colonic T cell populations in patients with CPI-colitis[19, 20, 35, 36, 37, 38], highlighting the fidelity of our disease model to the human disease. For the first time, we show that these effector T cells are functionally required for CPI colitis, since depletion of effector lymphocytes or IFNγ neutralization prevented disease.

Our study also provides some insights into the likely origin of pathogenic effector T cells. Both $CD4^+$ and $CD8^+$ clusters highly expressed *Cxcr6* but did not have increased expression of other markers of tissue

resident memory (T_{RM}) cells, such as *Itgae* or *Cd69*. These data are consistent with pathogenic $CD4^+$ and $CD8^+$ T cells arising from T_{RM} cells, especially since blockade of newly arriving α4β7 expressing lymphocytes failed to prevent colitis. These data are consistent with human scRNA-seq data showing that proliferating T cell clusters in CPI-colitis have lower expression of *Itgae* or *Cd69* but share TCR clonotypes with T_{RM} populations[19].

Another important characteristic of the IFNγ producing, polyfunctional T cell lineages identified in this study is that they significantly upregulated multiple costimulatory and coinhibitory receptors, indicating that these cells are very tightly regulated. This phenomenon has also been observed in the expanded T cell populations described in patients with CPI-colitis [19, 20]. We hypothesize that under physiological circumstances these potentially pathogenic cells are keep in check by engagement of immune checkpoint molecules with their natural ligands that are expressed in the gut. However, in patients undergoing checkpoint blockade, these crucial regulatory mechanisms are lost, and these potentially pathogenic effector cells escape repression enabling them to mediate disease. Given that these cells also express high levels of co-stimulatory molecules, they may be pre-primed for rapid activation and induction of pro-inflammatory effector pathways when regulation by the high levels of checkpoint molecules that they express is lost. Notably, CTLA-4 was one of the most highly expressed immune checkpoint molecules in both $CD4^+$ and $CD8^+$ T cells and was expressed at higher levels that PD-1, indicating that CTLA-4 may be especially important in restraining the pathogenic potential of these cells. Notably, cancer patients treated with anti-CTLA-4 antibodies have a much greater incidence of colitis than patients treated with anti-PD-1 antibodies.

Computational approaches predicted several cytokines, including IL23 as a potentially important upstream regulators of mucosal T cells in CPI-colitis. Here, we show that IL23 blockade, or genetic ablation, reduced pathogenic cytokine production by $CD4^+$ T cells, but not $CD8^+$ T cells in CPI-colitis, and significantly attenuated disease development. Notably, targeting IL23 did not completely prevent colitis, probably because pathogenic cytokine production was only reduced in $CD4^+$ T cells, but not $CD8^+$ T cells, which also likely contribute to colitis. Nevertheless, IL23 is a plausible and attractive target for CPI colitis. As well as being highly expressed in the colon of patients with CPI-colitis[39], its receptor (IL23R) is also expressed by multiple T cell clusters identified in single cell sequencing experiments of patients with CPI colitis [19]. Notably, mucosal T_{RM} cells also have increased expression of the IL23R[40]. IL23 plays an important role in other immune-mediated inflammatory diseases, especially at the barrier surfaces, and clinical reagents targeting this cytokine are already in advanced clinical development for conventional IBD, with promising results [41, 42]. IL23 blockade is also unlikely to impede systemic, anti-cancer immunity, and neutralization of the IL23 might even promote favourable cancer outcomes [43, 44, 45]. A case report of successful treatment of two cases of CPI-colitis following treatment with ustekinumab [46], which blocks the p40 subunit, common to both IL12 and IL23, further support the rationale for this approach. Other potentially targetable cytokines implicated in causal network analysis include IL7, IL15 and IL18. One of the key transcriptional regulators predicted to activate the gene expression changes observed in

polyfunctional mucosal lymphocytes was NFATc2, which notably is also highly upregulated in the colon of patients with CPI-colitis. Notably, calcineurin inhibitors, that target NFATc2 may be effective in patients with refractory CPI-colitis [47, 48].

In agreement with observations in human disease, susceptibility to CPI-induced colitis is dependent on the composition of the intestinal microbiota [21, 22, 23, 24]. The barrier surfaces, and the colon in particular, are challenged with maintaining immunological restraint against a multitude of different commensal bacteria that vary across individuals and time [49], whilst remaining poised to repel invading pathogens. In our data, transcriptomic analysis of the colon following colonization with a colitis permissive microbiota did trigger activation of some immune pathways, however, in the presence of intact immune checkpoint regulation overt colitis was averted. However, when these key checkpoints are inhibited, dysbiosis primes unchecked activation of polyfunctional, cytotoxic lymphocyte responses. Accordingly, immune checkpoint molecules are likely important immune rheostats in the regulation of host perception of the microbial colonization in the colon. Indeed, patients with germline deletions in the *CTLA4* gene spontaneously develop severe enterocolitis [50, 51].

In conclusion, this study provides new mechanistic insights into immune regulation at the mucosal barrier surfaces with important implications for the prevention and treatment of CPI-induced autoimmunity. In the context of a colitis permissive intestinal microbiota, combination immune checkpoint blockade with anti-CTLA-4 and anti-PD-1 results in the emergence of IL23-dependent, polyfunctional, cytolytic, $CD4^+$ and T cells responses that are functionally in CPI-colitis development. Effective strategies to target these pathogenic effector cells could herald improved clinical outcomes for patients affected by this severe, immune-mediated complication of life saving CPI therapy.

Materials And Methods

Animal Husbandry

C57BL/6 and Balb/c wild type mice (both Charles River) and *IL23*$^{-/-}$ mice (ModelOrganisms) were sourced commercially. TRUC mice have been described previously [25, 26, 52]. All mice were housed in specific pathogen–free facilities at King's College London Biological Services Unit, Imperial Hammersmith CBS, or Charles River Laboratories. All animal experiments were performed in accredited facilities in accordance with the UK Animals (Scientific Procedures) Act 1986 (Home Office Licence Numbers PPL: 70/6792, 70/8127 and 70/7869).

Isolation of cells

Mouse colons were excised and placed in cold Phosphate Buffered Saline (PBS) solution. Colonic lamina propria mononuclear cells (cLPMCs) leukocytes were isolated, as described previously [26, 52]. Briefly, the epithelium was removed in HBSS (Invitrogen) supplemented with 5mM of EDTA and 10mM HEPES

(Fisher Scientific). The tissue was digested in HBSS with 2% FCS and supplemented with 0.5mg/ml collagenase D, 10µg/ml DNase I and 1.5mg/ml dispase II (all Roche). The digested lymphocyte-enriched population was harvested using a 40%-80% Percoll (GE Healthcare) gradient centrifugation.

Flow Cytometry

Single suspension extracted cells, as described above, were plated into flow cytometry tubes (Sarstedt) at a concentration of 1 x 10^6 per ml. Cells were stimulated with 50ng/ml phorbol 12-myristate 13-acetate (PMA), 1µg/ml ionomycin, 2µM monensin (all Sigma Aldrich) for 3-4 hours as indicated. (Sigma Aldrich) FcR receptor blocking antibodies were added before staining with antibodies. Surface staining antibodies were added with live/dead stain (Invitrogen). For intracellular staining, cells were fixed and permeabilised using the Foxp3 fixation/permeabilization buffer kit (Thermo Fisher) according to the manufacturer's instructions. Samples were acquired using a BD LSRFortessa (BD Biosciences). Sample data was recorded in FCS 3.0 data format using BD FACSDiva 6.0 software (BD Biosciences). Analysis of the data was performed using FlowJo software (Treestar Inc., Ashland, OR, USA).

Histology

Whole mouse colon samples were rolled using the swiss roll technique and fixed in 10% paraformaldehyde and embedded in paraffin blocks. 3µm sections were stained for haemotoxylin and eosin.

In vivo murine antibody and faecal microbiota transplant treatment

Faecal content extracted from the caecum of TRUC mice was spun down and reconstituted in sterile PBS with 25% glycerol and then 200µl was orally gavaged into mice. Mice treated with immune checkpoint blockade drugs were intraperitoneally administered anti-CTLA-4 (9H10, BioXCell) using doses of 200µg and anti-PD-1 (RMP1-14, BioXCell) at a dose of 250µg once per week [53]. Mice treated with depleting antibodies were intraperitoneally administered once a week, at the same time of giving anti-CTLA-4 and anti-PD-1 antibodies, either 500µg anti-CD90.2 (Thy1.2, 30H12, BioXCell) or 150µg anti-IL-23(p19) (G23-8, BioXCell). Control-isotype clones used were 2A3 (rat IgG2a) and HRPN (rat IgG1).

Bulk RNA-seq data analysis

RNA extractions methods can be found in the Supplementary Materials and Methods. The quality of the raw library files was inspected with fastQC. Raw reads were trimmed and filtered to remove adaptor

contamination and poor-quality bases using trimmomatic [54]. The resulting read files were mapped to the GRCm38 (mouse) or GRCh38 (human) genome assembly using Hisat2 [55] with default parameters. The number of reads mapping to the genomic features annotated in Ensembl [56] with a MAPQ score higher than or equal to 10 was calculated for all samples using htseq-count [57] with default parameters. Differential expression analysis between sample groups was performed in R using the Wald test as implemented in the DESeq2 package [58]. P-values were adjusted for multiple testing with the Benjamini and Hochberg procedure [59]. The P- and corresponding FDR values were re-estimated empirically with fdrtool [60], when the histograms of the initial P-value distributions showed that the assumptions of the test were not met.

Droplet-based single cell RNA sequencing

Colonic lamina propria cells from mice were initially sorted using a FACS Aria machine (BD Biosciences) based on live $CD45^+$ gates and taken immediately to be run on the 10x. Cells were suspended at $1x10^6$/mL in PBS and 10,000 cells were loaded onto the Chromium™ Controller instrument within 15 min after completion of the cell suspension preparation using GemCode Gel Bead and Chip, all from 10x Genomics (Pleasanton, CA), and following the manufacturer's recommendations. Briefly, cells were partitioned into Gel Beads in Emulsion in the Chromium™ Controller instrument where cell lysis and barcoded reverse transcription of RNA occurred. Libraries were prepared using 10x Genomics Library Kits and sequenced on an Illumina NextSeq500 according to the manufacturer's recommendations. Read depth of more than 200 million reads per library, or an approximate average of 10,000 reads per cell was obtained.

Statistical analysis

Results are expressed as median ± IQR. Data were analysed using Two-way Student's t-test, Two-way Mann-Whitney U test, Two-Way ANOVA Kruskal-Wallis test, as appropriate, using GraphPad Prism 10.0 (GraphPad Inc., USA).

Declarations

Acknowledgments

The authors acknowledge *Rosalind* (https://rosalind.kcl.ac.uk), the research computing facility at King's College London, which is delivered in partnership with the NIHR BRC Biomedical Research Centres at South London & Maudsley and Guy's & St. Thomas' NHS Foundation Trusts, and part-funded by capital equipment grants from the Maudsley Charity (award 980) and Guy's & St. Thomas' Charity (TR130505). We also would like to acknowledge the BRC FlowCore at King's College London and the MRC LMS

FlowCore facility at Imperial College London. The views expressed are those of the author(s) and not necessarily those of the NHS, the NIHR, Imperial College London, King's College London, or the Department of Health and Social Care. We also acknowledge Novogene for the RNA sequencing and the BRC Genomics Facility at King's College London for the 10X Genomics single-cell RNA sequencing.

Funding support

NP was funded by the Wellcome Trust (WT101159) and the Imperial National Institute for Health Research (NIHR) Biomedical Research Centre (BRC). Infrastructure support for this research was provided by the NIHR Imperial Biomedical Research Centre (BRC). GML was funded by grants awarded by the Wellcome Trust (091009) and the Medical Research Council (MR/M003493/1 and MR/K002996/1). MM was supported by the UKRI Biotechnological and Biosciences Research Council (BBSRC) Norwich Research Park Biosciences Doctoral Training Partnership (BB/S50743X/1). The work of TK was supported by the Earlham Institute (Norwich, UK) in partnership with the Quadram Institute (Norwich, UK) and strategically supported by a UKRI BBSRC UK grant (BB/ CSP17270/1) and a BBSRC ISP grant for Gut Microbes and Health BB/ R012490/1 and its constituent projects, BBS/E/F/ 000PR10353 and BBS/E/F/000PR10355.

Author Contributions

Study concept and design (NP, JWL), acquisition of data (JWL, DC, MM, JYXS, JLA, HK, RG), data analysis and interpretation (JWL, DC, JYXS, JLA, JMB, MM, RG, NP), technical support (JYXS, JLA, JM, MM, TK, HK, RCS, ZL, HI, JM), and obtained funding (NP, GML, TK). The manuscript was drafted by JWL, edited by NP, and was critically reviewed by all authors.

Conflict of Interest

The authors declare no conflicting interests.

References

1. Phan GQ, *et al.* Cancer regression and autoimmunity induced by cytotoxic T lymphocyte-associated antigen 4 blockade in patients with metastatic melanoma. *Proc Natl Acad Sci U S A* **100**, 8372–8377 (2003).
2. Hodi FS, *et al.* Improved survival with ipilimumab in patients with metastatic melanoma. *N Engl J Med* **363**, 711–723 (2010).

3. Robert C, *et al.* Pembrolizumab versus Ipilimumab in Advanced Melanoma. *N Engl J Med* **372**, 2521–2532 (2015).
4. Antonia SJ, *et al.* Nivolumab alone and nivolumab plus ipilimumab in recurrent small-cell lung cancer (CheckMate 032): a multicentre, open-label, phase 1/2 trial. *Lancet Oncol* **17**, 883–895 (2016).
5. Cohen EEW, *et al.* Pembrolizumab versus methotrexate, docetaxel, or cetuximab for recurrent or metastatic head-and-neck squamous cell carcinoma (KEYNOTE-040): a randomised, open-label, phase 3 study. *Lancet* **393**, 156–167 (2019).
6. Motzer RJ, *et al.* Nivolumab plus Ipilimumab versus Sunitinib in Advanced Renal-Cell Carcinoma. *N Engl J Med* **378**, 1277–1290 (2018).
7. Larkin J, *et al.* Combined Nivolumab and Ipilimumab or Monotherapy in Untreated Melanoma. *N Engl J Med* **373**, 23–34 (2015).
8. Postow MA, *et al.* Nivolumab and ipilimumab versus ipilimumab in untreated melanoma. *N Engl J Med* **372**, 2006–2017 (2015).
9. Wolchok JD, *et al.* Nivolumab plus ipilimumab in advanced melanoma. *N Engl J Med* **369**, 122–133 (2013).
10. Khoja L, Day D, Wei-Wu Chen T, Siu LL, Hansen AR. Tumour- and class-specific patterns of immune-related adverse events of immune checkpoint inhibitors: a systematic review. *Ann Oncol* **28**, 2377–2385 (2017).
11. De Velasco G, *et al.* Comprehensive Meta-analysis of Key Immune-Related Adverse Events from CTLA-4 and PD-1/PD-L1 Inhibitors in Cancer Patients. *Cancer Immunol Res* **5**, 312–318 (2017).
12. Hassel JC, *et al.* Combined immune checkpoint blockade (anti-PD-1/anti-CTLA-4): Evaluation and management of adverse drug reactions. *Cancer Treat Rev* **57**, 36–49 (2017).
13. Del Castillo M, Romero FA, Arguello E, Kyi C, Postow MA, Redelman-Sidi G. The Spectrum of Serious Infections Among Patients Receiving Immune Checkpoint Blockade for the Treatment of Melanoma. *Clin Infect Dis* **63**, 1490–1493 (2016).
14. Favara DM, *et al.* Five-year review of corticosteroid duration and complications in the management of immune checkpoint inhibitor-related diarrhoea and colitis in advanced melanoma. *ESMO Open* **5**, (2020).
15. Faje AT, *et al.* High-dose glucocorticoids for the treatment of ipilimumab-induced hypophysitis is associated with reduced survival in patients with melanoma. *Cancer* **124**, 3706–3714 (2018).
16. Arbour KC, *et al.* Impact of Baseline Steroids on Efficacy of Programmed Cell Death-1 and Programmed Death-Ligand 1 Blockade in Patients With Non-Small-Cell Lung Cancer. *J Clin Oncol* **36**, 2872–2878 (2018).
17. Ibraheim H, *et al.* Systematic review with meta-analysis: effectiveness of anti-inflammatory therapy in immune checkpoint inhibitor-induced enterocolitis. *Alimentary pharmacology & therapeutics* **52**, 1432–1452 (2020).

18. Alexander JL, *et al.* Clinical outcomes of patients with corticosteroid refractory immune checkpoint inhibitor-induced enterocolitis treated with infliximab. *Journal for immunotherapy of cancer* **9**, (2021).
19. Luoma AM, *et al.* Molecular Pathways of Colon Inflammation Induced by Cancer Immunotherapy. *Cell*, (2020).
20. Sasson SC, *et al.* Interferon-Gamma-Producing CD8(+) Tissue Resident Memory T Cells Are a Targetable Hallmark of Immune Checkpoint Inhibitor-Colitis. *Gastroenterology* **161**, 1229-1244.e1229 (2021).
21. Chaput N, *et al.* Baseline gut microbiota predicts clinical response and colitis in metastatic melanoma patients treated with ipilimumab. *Ann Oncol* **28**, 1368–1379 (2017).
22. Vetizou M, *et al.* Anticancer immunotherapy by CTLA-4 blockade relies on the gut microbiota. *Science* **350**, 1079–1084 (2015).
23. Dubin K, *et al.* Intestinal microbiome analyses identify melanoma patients at risk for checkpoint-blockade-induced colitis. *Nat Commun* **7**, 10391 (2016).
24. Gopalakrishnan V, *et al.* Gut microbiome modulates response to anti-PD-1 immunotherapy in melanoma patients. *Science* **359**, 97–103 (2018).
25. Garrett WS, *et al.* Communicable ulcerative colitis induced by T-bet deficiency in the innate immune system. *Cell* **131**, 33–45 (2007).
26. Powell N, *et al.* The transcription factor T-bet regulates intestinal inflammation mediated by interleukin-7 receptor+ innate lymphoid cells. *Immunity* **37**, 674–684 (2012).
27. Powell N, *et al.* British Society of Gastroenterology endorsed guidance for the management of immune checkpoint inhibitor-induced enterocolitis. *Lancet Gastroenterol Hepatol* **5**, 679–697 (2020).
28. Stavnezer J. Complex regulation and function of activation-induced cytidine deaminase. *Trends Immunol* **32**, 194–201 (2011).
29. Jackson B, *et al.* Late cornified envelope family in differentiating epithelia--response to calcium and ultraviolet irradiation. *The Journal of investigative dermatology* **124**, 1062–1070 (2005).
30. Niehues H, *et al.* Psoriasis-Associated Late Cornified Envelope (LCE) Proteins Have Antibacterial Activity. *The Journal of investigative dermatology* **137**, 2380–2388 (2017).
31. Rukmangadachar LA, *et al.* Proteome analysis of the macroscopically affected colonic mucosa of Crohn's disease and intestinal tuberculosis. *Scientific reports* **6**, 23162 (2016).
32. Taman H, Fenton CG, Hensel IV, Anderssen E, Florholmen J, Paulssen RH. Transcriptomic Landscape of Treatment-Naïve Ulcerative Colitis. *Journal of Crohn's & colitis* **12**, 327–336 (2018).
33. Perez-Ruiz E, *et al.* Prophylactic TNF blockade uncouples efficacy and toxicity in dual CTLA-4 and PD-1 immunotherapy. *Nature* **569**, 428–432 (2019).
34. Haeryfar SM, Al-Alwan MM, Mader JS, Rowden G, West KA, Hoskin DW. Thy-1 signaling in the context of costimulation provided by dendritic cells provides signal 1 for T cell proliferation and cytotoxic

effector molecule expression, but fails to trigger delivery of the lethal hit. *Journal of immunology (Baltimore, Md*: 1950) **171**, 69-77 (2003).

35. Hashimoto K, *et al.* Single-cell transcriptomics reveals expansion of cytotoxic CD4 T cells in supercentenarians. *Proc Natl Acad Sci U S A* **116**, 24242–24251 (2019).
36. Appay V, *et al.* Characterization of CD4(+) CTLs ex vivo. *J Immunol* **168**, 5954–5958 (2002).
37. Śledzińska A, *et al.* Regulatory T Cells Restrain Interleukin-2- and Blimp-1-Dependent Acquisition of Cytotoxic Function by CD4(+) T Cells. *Immunity* **52**, 151-166.e156 (2020).
38. Wei SC, *et al.* Distinct Cellular Mechanisms Underlie Anti-CTLA-4 and Anti-PD-1 Checkpoint Blockade. *Cell* **170**, 1120-1133.e1117 (2017).
39. Perez-Ruiz E, *et al.* Prophylactic TNF blockade uncouples efficacy and toxicity in dual CTLA-4 and PD-1 immunotherapy. *Nature* **569**, 428–432 (2019).
40. Bartolomé-Casado R, *et al.* Resident memory CD8 T cells persist for years in human small intestine. *The Journal of experimental medicine* **216**, 2412–2426 (2019).
41. Sands BE, *et al.* Efficacy and Safety of MEDI2070, an Antibody Against Interleukin 23, in Patients With Moderate to Severe Crohn's Disease: A Phase 2a Study. *Gastroenterology* **153**, 77-86 e76 (2017).
42. Feagan BG, *et al.* Induction therapy with the selective interleukin-23 inhibitor risankizumab in patients with moderate-to-severe Crohn's disease: a randomised, double-blind, placebo-controlled phase 2 study. *Lancet (London, England)* **389**, 1699–1709 (2017).
43. Zhang L, *et al.* IL-23 selectively promotes the metastasis of colorectal carcinoma cells with impaired Socs3 expression via the STAT5 pathway. *Carcinogenesis* **35**, 1330–1340 (2014).
44. Uhlig HH, *et al.* Differential activity of IL-12 and IL-23 in mucosal and systemic innate immune pathology. *Immunity* **25**, 309–318 (2006).
45. Langowski JL, *et al.* IL-23 promotes tumour incidence and growth. *Nature* **442**, 461–465 (2006).
46. Thomas AS, Ma W, Wang Y. Ustekinumab for Refractory Colitis Associated with Immune Checkpoint Inhibitors. *The New England journal of medicine* **384**, 581–583 (2021).
47. Beardslee T, Draper A, Kudchadkar R. Tacrolimus for the treatment of immune-related adverse effects refractory to systemic steroids and anti-tumor necrosis factor α therapy. *J Oncol Pharm Pract* **25**, 1275–1281 (2019).
48. Rao A, Luo C, Hogan PG. Transcription factors of the NFAT family: regulation and function. *Annu Rev Immunol* **15**, 707–747 (1997).
49. Lozupone CA, Stombaugh JI, Gordon JI, Jansson JK, Knight R. Diversity, stability and resilience of the human gut microbiota. *Nature* **489**, 220–230 (2012).
50. Schubert D, *et al.* Autosomal dominant immune dysregulation syndrome in humans with CTLA4 mutations. *Nat Med* **20**, 1410–1416 (2014).
51. Kuehn HS, *et al.* Immune dysregulation in human subjects with heterozygous germline mutations in CTLA4. *Science* **345**, 1623–1627 (2014).

52. Powell N, *et al.* Interleukin 6 Increases Production of Cytokines by Colonic Innate Lymphoid Cells in Mice and Patients With Chronic Intestinal Inflammation. *Gastroenterology* **149**, 456-467 e415 (2015).
53. Wei SC, *et al.* Distinct Cellular Mechanisms Underlie Anti-CTLA-4 and Anti-PD-1 Checkpoint Blockade. *Cell* **170**, 1120-1133.e1117 (2017).
54. Bolger AM, Lohse M, Usadel B. Trimmomatic: a flexible trimmer for Illumina sequence data. *Bioinformatics* **30**, 2114–2120 (2014).
55. Kim D, Langmead B, Salzberg SL. HISAT: a fast spliced aligner with low memory requirements. *Nat Methods* **12**, 357–360 (2015).
56. Yates AD, *et al.* Ensembl 2020. *Nucleic acids research* **48**, D682-d688 (2020).
57. Anders S, Pyl PT, Huber W. HTSeq–a Python framework to work with high-throughput sequencing data. *Bioinformatics* **31**, 166–169 (2015).
58. Love MI, Huber W, Anders S. Moderated estimation of fold change and dispersion for RNA-seq data with DESeq2. *Genome Biol* **15**, 550 (2014).
59. Hochberg Y, Benjamini Y. More powerful procedures for multiple significance testing. *Stat Med* **9**, 811–818 (1990).
60. Strimmer K. A unified approach to false discovery rate estimation. *BMC Bioinformatics* **9**, 303 (2008).

Figures

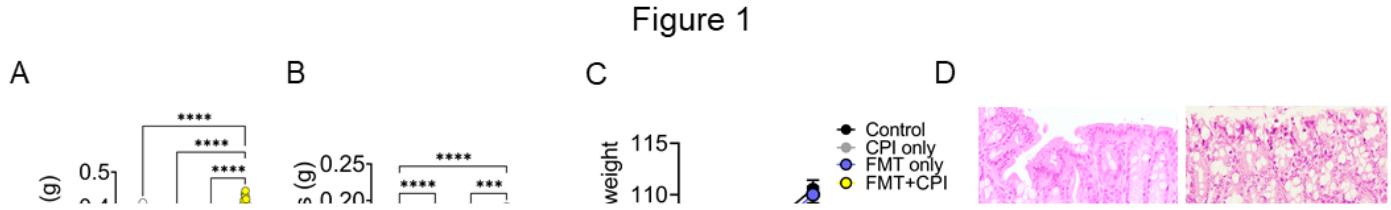

Figure 1

Intestinal microbiota regulates susceptibility to CPI-induced colitis

(A) Colon mass, (B) spleen mass and (C) change in body weight in wildtype Balb/C mice without treatment (Control, n=61), treatment with combination anti-CTLA4/anti-PD-1 (CPI, n=25), treatment with faecal microbiota (FMT, n=29) and mice treated with both CPI and FMT (n=143). (D) Representative colon sections cut at 3µm thick FFPE from control, CPI, FMT and CPI+FMT treated wildtype Balb/C mice stained with H&E (Leica). (E) Representative flow cytometry plot showing the $CD4^+$ and $CD8^+$ T cell gating. (F) Number of $CD4^+$ T cells from Control (n=6), CPI (n=6), FMT (n=6) and CPI+FMT (n=14) treated

wildtype Balb/C mice. (G) Number of $CD8^+$ T cells from Control (n=6), CPI (n=6), FMT (n=6) and CPI+FMT (n=14) treated wildtype Balb/C mice. (H) Representative flow cytometry plot showing Gr-1^{hi} neutrophils from Control, CPI, FMT and CPI+FMT treated wildtype Balb/C mice. (I) Number of Gr-1^{hi} neutrophils from Control (n=20), CPI (n=18), FMT (n=15) and CPI+FMT (n=68) treated wildtype Balb/C mice. * P<0.05 ** P<0.01 *** P<0.001 **** P<0.0001 2-sided Kruskal-Wallis Test showing median.

Figure 2

Transcriptome analysis shows colonic epithelial dysfunction and activation of T cells, cytotoxicity, and immune compartments in mice with CPI-induced colitis

(A) Heatmap of the z-score transformed FPKM values of the DEGs (FDR < 0.05) identified by comparing the expression profiles of whole colon biopsies from mice with only CPI treatment (n=4), only FMT (n=3) or with both CPI+FMT (n=3) against control mice (n=4). (B) Volcano plot highlighting the DEGs (FDR < 0.05) from the comparison of RNA samples from mice treated with both CPI+FMT (n=3) versus control mice (n=4). Positive log fold changes indicate over-expression in treated mice, while negative log fold changes indicate up-regulation in wildtype mice. (C) The 15 most significantly upregulated genes involved in epithelial function, extracellular matrix regulation and anti-microbial responses in the distal colon of mice with CPI-induced colitis (n=3) in comparison with control mice (n=4). (D) Gene expression changes in the distal colon of mice with CPI-induced colitis (n=3) in comparison with control mice (n=4) were used to identify which biological pathways were significantly impacted, using IPA Canonical Pathways. (E) Significant fold changes to genes associated with biological functions and diseases in the colon of mice with CPI-induced colitis (n=3) in comparison with control mice (n=4) were identified using IPA Downstream Effect Analysis. (F) Upstream regulators predicted to control the gene expression changes observed in the colon of mice treated with CPI (n=4), FMT (n=3) and both treatments together (CPI+FMT, n=3), in comparison with control mice (n=4) were identified using IPA Upstream Regulator Analysis.

Figure 3

Transcriptomic landscape of colonic lymphocytes in CPI-induced colitis at single cell resolution

(A) t-SNE plots of the 26 lymphocyte populations labelled according to Louvain clustering, coloured based on SingleR cell-type assignments and split by the two conditions under consideration. (B) Circular bar plot of the log fold changes in cell abundance, differentially expressed transcripts ranked by

increasing log fold change and coloured by estimated false discovery rate (FDR) and canonical pathways, identified using IPA Canonical Pathway, significantly impacted in colonic T cells, (C) B cells and (D) ILCs in mice with CPI-induced colitis (n=3) vs control mice (n=4) (E) Violin plots showing the expression levels of cytokines across T cell, B cell and ILC clusters in mice with CPI-induced colitis.

Figure 4

CPI-induced colitis exhibits a profound and increased cytotoxic phenotype

(A) t-SNE plot showing the increased occurrence of *Ifng* and (B) *Gzmb* expressing cells in CPI-induced colitis (n=3) vs control samples (n=4) in colonic T cell clusters. (C) Heatmap of cytokine and chemokine expression shown by log_2 fold changes between CPI-induced colitis (n=3) and control samples (n=4) in colonic $CD4^+$ and $CD8^+$ T cell clusters. (D) Representative flow cytometry histograms and bubble plots showing the percentage of granzyme B, IFNγ and perforin expressing $CD3^+$ $CD4^+$ T cells and (E) $CD3^+$ $CD8^+$ T cells in mice with CPI-induced colitis (n=16) and control mice (n=16). (F) Overlapping biological pathways which were significantly impacted shown as a network, using IPA Canonical Pathways, in *Ifng*-expressing $CD4^+$ T cells in CPI colitis (n=3) in comparison with *Ifng*-expressing lymphocytes in control mice (n=4). (G) Colon mass of CPI-colitis mice treated with an isotype control (n=16) or anti-IFNγ (anti-IFNγ) (n=16) **** P<0.0001 2-sided Mann-Whitney U Test showing median.

Figure 5

CPI-induced colitis is mediated by CD90 activated T cells

(A) Heatmap of co-stimulatory and co-inhibitory expression from *Ifng*$^+$ expressing $CD4^+$ and $CD8^+$ T cells in comparison to *Ifng*$^-$-expressing $CD4^+$ and $CD8^+$ T cells. (B) Representative flow cytometry histogram showing increased percentage of CD90 expressing $CD4^+$ and $CD8^+$ T cells following induction of CPI-colitis, in comparison with control mice. (C) Bar chart showing increased CD90 mean fluorescent intensity (MFI) from $CD4^+$ and $CD8^+$ T cells following induction of CPI-colitis (n=6), in comparison with control mice (n=4). (D) Representative flow plots showing the $CD90^{hi}$ production of cytotoxic polyfunctional IFNγ/TNFα $CD4^+$ and $CD8^+$ T cells. (E) Representative flow cytometry plot and (F) number of $CD90^+$ cells in CPI-colitis mice treated with an isotype control (n=8) or CD90 depleting antibody (n=8). (G) Colon mass and (H) Gr-1^{hi} neutrophil counts in CPI-colitis mice treated with an isotype control (n=8) or CD90 depleting antibody (n=8). (I) Heatmap of chemokines and gut homing gene expression from *Ifng*$^+$ expressing $CD4^+$

and $CD8^+$ T cells in comparison to *Ifng*$^-$-expressing $CD4^+$ and $CD8^+$ T cells. (J) Percentage of $CD3^+$ $\alpha4\beta7^+$ in the colon and mesenteric lymph node (mLN), (K) colon mass and (L) number of Gr-1^{hi} neutrophils in CPI-colitis mice treated with an isotype control (n=8) or anti-α4β7 depleting antibody (n=8). * P<0.05 *** P<0.001 two-sided Mann-Whitney U test.

Figure 6

IL23 blockade attenuates the development of CPI-colitis

(A) Network analysis, using Enhanced Causal Network using Qiagen IPA, of predicted upstream regulators of *Ifng*-expressing $CD4^+$ T cell in CPI-colitis. Multiple cytokines, transmembrane receptors and transcriptional regulators were predicted to significantly (FDR<0.05) regulate *Ifng*-expressing $CD4^+$ T cell. (B) Representative flow cytometry plot and (C) percentage of $IFN\gamma^+/TNF\alpha^+$ $CD4^+$ T cells from CPI-colitis mice treated with an isotype control (n=7) or an IL-23 blocking antibody (n=8). (D) Colon mass and (E) Gr-1^{hi} neutrophil counts in either control mice (n=12) or CPI-colitis mice treated with an isotype control (n=23) or an IL-23 blocking antibody (n=24). (F) Colon mass and (G) Gr-1^{hi} neutrophil counts in either wildtype mice (n=17) or *Il23*$^{-/-}$ mice (n=20) treated with CPI-colitis. (H) Representative flow cytometry plot and (I) percentage of $IFN\gamma^+/TNF\alpha^+$ $CD4^+$ T cells from CPI-colitis treated wildtype mice (n=8) or *Il23*$^{-/-}$ mice (n=12). (J) Significant gene expression changes in biopsies of CPI-colitis patients (n=4) compared to healthy controls (n=4) for selected cytokines, cytokine receptors, transcription factors and enzymes. (K) Network analysis of *Ifng*-expressing $CD4^+$ T cell in CPI-colitis showing the significant direct genes linking between *Il23r* to *Ifng*.

* P<0.05 ** P<0.01 *** P<0.001 **** P<0.0001 two-sided Mann-Whitney U test for Colon mass in F, Gr-1^{hi} and percentage of $IFN\gamma^+/TNF\alpha^+$ $CD4^+$ T cells or Kruskal-Wallis test for colon mass in D.

Supplementary Files

This is a list of supplementary files associated with this preprint. Click to download.

- SupplementaryTable1.docx
- SupplementaryMaterial.pdf